

Impurities in a trapped 1D Bose gas of arbitrary interaction strength: localization-delocalization transition and absence of self-localization

Dennis Breu, Eric Vidal Marcos, Martin Will, and Michael Fleischhauer

*Department of Physics and Research Center OPTIMAS,
University of Kaiserslautern-Landau, 67663 Kaiserslautern, Germany*

(Dated: August 22, 2024)

We discuss impurities in a trapped one-dimensional Bose gas with arbitrary boson-boson and boson-impurity interactions. To fully account for quantum effects, in particular in the regime of strong boson-boson interactions, we employ numerical simulations based on the density-matrix renormalization group (DMRG) and analytic approximations exploiting the mapping to weakly interacting fermions. Mobile impurities in a box potential undergo a phase transition between a delocalized state and a solution localized at one of the potential edges upon increasing the impurity-boson interaction. While a mean-field ansatz based on coupled Gross-Pitaevski – Schrödinger equations gives reasonable predictions of this transition, it also predicts the existence of a self-localized polaron solution, which we show to be an artifact of the underlying decoupling approximation. This demonstrates that impurity-boson correlations are important even in the limit of weak boson-boson interactions, where mean-field approaches are expected to work well. Furthermore we calculate the energy of a single polaron formed by a heavy impurity for arbitrary interaction strengths and give analytical approximations for large but finite boson-boson couplings. Finally we numerically determine the polaron-polaron interaction potential in Born-Oppenheimer approximation, which in the Tonks gas limit is oscillatory due to Friedel oscillations in the Bose gas.

I. INTRODUCTION

Quasi particles formed by quantum impurities immersed in a many-body environment play a key role for the understanding of transport phenomena [1]. Furthermore the interaction of quasi particles mediated by the host medium forms the basis of many important many-body phenomena in condensed-matter physics [2–5]. In recent years the possibility to experimentally investigate impurities in quantum fluids, such as Bose-Einstein condensates (BEC) of atoms has renewed the interest in these quasi-particles, called Bose polarons. An important difference between Bose polarons in ultra-cold quantum gases and the Landau-Pekar polaron [6, 7] introduced to model electrons interacting with the lattice vibrations of a solid is the large compressibility of the BEC. As a consequence the standard model for polarons in solids, the Fröhlich model [8], which describes the polaron as interaction of the impurity with phonon excitations, is only suitable for weak boson-boson and weak impurity-boson interactions [9]. In this limit the condensate can be considered undepleted and the role of lattice vibrations is taken over by the Bogoliubov phonons.

For stronger interactions the back-action of the impurity to the condensate needs to be taken into account, while keeping correlations between impurity and bosons. For translational invariant systems this can be done by means of a Lee-Low-Pines (LLP) transformation [10], which decouples the impurity motion from the many-body problem of interacting bosons. For weak boson-boson interactions the latter can then be treated rather accurately in a mean-field description for arbitrary strength of the impurity-boson coupling [11–15].

In an inhomogeneous Bose gas and for repulsive impurity-boson interactions, the polaron can localize

in density minima of the Bose gas and, similarly to phase separation in multi-component condensates [16], a localization-delocalization transition can occur. Due to the absence of translational invariance the LLP decoupling does not work here, however. Instead another mean-field ansatz is often used, which in addition neglects correlations between impurity and bosons and results in a coupled Gross-Pitaevski and Schrödinger equation for the condensate and the impurity respectively [17–22]. This decoupling mean-field approach (DMF) however also predicts a localization transition to occur in translationally invariant systems. In analogy to impurities in liquid ^4He [23, 24], a single atom can become *self-trapped* in a localized distortion of the condensate created by the impurity [17–22] thereby spontaneously breaking translational invariance. In 2D and 3D a critical interaction strength is needed for such a self-trapped polaron to exist, but in 1D arbitrarily small impurity-boson interactions are sufficient [21, 22].

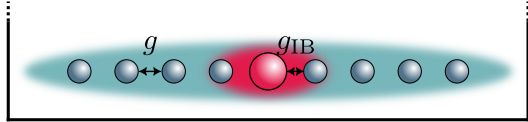


Figure 1. Mobile quantum impurity in a one-dimensional, interacting Bose gas, trapped in a box potential. Boson-boson interaction is characterized by coupling strength g and the impurity interacts with the Bose gas with strength g_{IB} .

In the present paper we analyze the role of quantum fluctuations to localization-delocalization transitions of impurities in BECs. To this end we consider a mobile impurity of finite mass M in a one-dimensional condensate and employ numerical simulations based on the density-matrix renormalization group (DMRG) [25, 26]. Further-

more we consider a box potential, see Fig. 1, to explicitly break translational invariance. For such a system decoupling mean-field theory predicts a reentry transition from a *self-localized* polaron at the trap center to a polaron localized at the potential edge upon changing the impurity-boson coupling strength. We numerically determine the ground-state phase diagram taking quantum fluctuations into account and observe instead only a phase transition between a fully *delocalized* phase for small values of the impurity-boson coupling g_{IB} and a localized phase near one of the edges. While the latter is in qualitative agreement with DMF predictions, our simulations show that there is no self-trapped solution in the full quantum problem.

We proceed by considering a heavy impurity $M \gg m$ and calculate the polaron energy as function of impurity-boson coupling for different boson-boson interaction strength ranging from the Bogoliubov regime to the Tonks-gas regime of (nearly) impenetrable bosons. Making use of the mapping between strongly interacting bosons and weakly interacting fermions, we derive analytical approximations of the polaron energy which agree very well with the numerical DMRG data. Finally we calculate the effective interaction potential between two heavy impurities in Born-Oppenheimer approximation for short distances. In a weakly interacting Bose gas the potential is monotonous and has a linear slope for small distances [13]. In the Tonks gas limit of impenetrable bosons the potential is modified by oscillations due to Friedel-like density oscillations of the hard-core bosons.

The paper is organized as follows: In Sec. II we introduce the model and briefly discuss the numerical methods used. Then we discuss a finite-mass impurity in a one-dimensional Bose gas in a trap potential in Sec. III. Finally we discuss the properties of a single polaron formed by a heavy impurity in a strongly interacting Bose gas in Sec. IV and the interaction between two heavy polarons in Born-Oppenheimer approximation in Sec. V.

II. MODEL AND NUMERICAL METHOD

A. Model

The Hamiltonian describing a single quantum impurity in an interacting 1D Bose gas in a box potential of length L has the form ($\hbar = 1$)

$$\hat{H} = \frac{\hat{p}^2}{2M} + \int_{-L/2}^{L/2} dx \hat{\phi}^\dagger(x) \left[-\frac{\partial_x^2}{2m} + \frac{g}{2} \hat{\phi}^\dagger(x) \hat{\phi}(x) + g_{IB} \delta(x - \hat{r}) \right] \hat{\phi}(x), \quad (1)$$

where m (M) is the boson (impurity) mass and g (g_{IB}) the strength of the bose-bose (bose-impurity) s -wave interaction. \hat{p} and \hat{r} represent the momentum and position operators of the impurity in first quantization. $\hat{\phi}(x)$ is

the field operator for the bosons. The bosons and the impurity are trapped in an infinitely deep box potential, described by open boundary conditions at $x = \pm L/2$. To quantify the internal interaction strength of the 1D Bose gas we use the unitless Tonks parameter

$$\gamma = \frac{gm}{n_0}, \quad (2)$$

where n_0 is the mean particle density of bosons in the system. The Tonks parameter gives a relation between the interaction ($\propto gn_0^2$) and kinetic energies ($\propto n_0^3/m$) of the bosons. A large value of γ corresponds to strong boson-boson interactions. For $\gamma \ll 1$ and below a critical temperature a quasi condensate forms. (True condensation is not possible due to the Mermin-Wagner-Hohenberg theorem [27, 28].) For $\gamma \rightarrow \infty$ the bosons become impenetrable hard-core bosons and can be mapped to free fermions [29].

B. DMRG simulation of quantum impurity in a 1D Bose gas

A powerful method to describe the ground-state of quantum many-body systems in 1D is the density matrix renormalization group (DMRG) [25]. The DMRG method was originally developed for lattice systems. It can also be applied to continuous models, however, e.g. using a proper discretization, which we apply here. To this end let us first look at the Hamiltonian where both bosons and the impurity are described in second quantization:

$$\hat{H} = \int dx \hat{\phi}^\dagger(x) \left[-\frac{\partial_x^2}{2m} + \frac{g}{2} \hat{\phi}^\dagger(x) \hat{\phi}(x) \right] \hat{\phi}(x) + \int dx \hat{\phi}_I^\dagger(x) \left[-\frac{\partial_x^2}{2M} + g_{IB} \hat{\phi}^\dagger(x) \hat{\phi}(x) \right] \hat{\phi}_I(x), \quad (3)$$

where $\hat{\phi}_I$ is the impurity field operator.

Discretization of the x -coordinate into a 1D lattice with lattice spacing Δx , the field operators can be replaced by creation and annihilation operators at position $x_i = i\Delta x$

$$\hat{\phi}(x_i) \rightarrow \frac{1}{\sqrt{\Delta x}} \hat{a}_i \quad \hat{\phi}_I(x_i) \rightarrow \frac{1}{\sqrt{\Delta x}} \hat{b}_i. \quad (4)$$

The second order derivative in eq. (3) can then be written as

$$\frac{\partial^2}{\partial x^2} \hat{\phi}(x) \approx \frac{\hat{a}_{i-1} - 2\hat{a}_i + \hat{a}_{i+1}}{\Delta x}, \quad (5)$$

and we set the hoppings which go from and to site 0 and $L + 1$ to 0. This is justified because our average system sizes exceed 400 lattice sites were the energy contributions from these hopping terms are small compared to the overall energy. By inserting these transformations

into eq. (3) one arrives at a tight-binding lattice Hamiltonian

$$\begin{aligned} \hat{H} = \sum_i & -J \left(\hat{a}_i^\dagger \hat{a}_{i+1} + \text{h.c.} \right) + 2J \hat{a}_i^\dagger \hat{a}_i \\ & + \frac{U}{2} \hat{a}_i^\dagger \hat{a}_i^\dagger \hat{a}_i \hat{a}_i \\ & - J_I \left(\hat{b}_i^\dagger \hat{b}_{i+1} + \text{h.c.} \right) + 2J_I \hat{b}_i^\dagger \hat{b}_i \\ & + U_I \hat{b}_i^\dagger \hat{a}_i^\dagger \hat{a}_i \hat{b}_i, \end{aligned} \quad (6)$$

where

$$J = \frac{1}{2m\Delta x^2}, \quad U = \frac{g}{\Delta x}, \quad (7)$$

$$J_I = \frac{1}{2M\Delta x^2}, \quad U_I = \frac{g_{IB}}{\Delta x}. \quad (8)$$

Here the terms containing $\hat{a}_i^\dagger \hat{a}_{i+1}$ ($\hat{b}_i^\dagger \hat{b}_{i+1}$) describe the hopping between lattice sites for the bosons (impurity) with hopping amplitude J (J_I). The diagonal terms $\sim \hat{a}_i^\dagger \hat{a}_i$ (or $\hat{b}_i^\dagger \hat{b}_i$) describe a local potential at site i for the bosons (impurity). The strength of this potential is also given by the hopping amplitude J (J_I). It doesn't effect the dynamics of the system but needs to be taken into account when calculating the ground state energy. The terms proportional to $\hat{a}_i^\dagger \hat{a}_i^\dagger \hat{a}_i \hat{a}_i$ ($\hat{b}_i^\dagger \hat{a}_i^\dagger \hat{a}_i \hat{b}_i$) relate to the interaction between the bosons (bosons and impurity). The strength of this interaction is given by U (U_I). A graphical illustration of the terms of Hamiltonian eq. (6) is given in Fig. 2a).

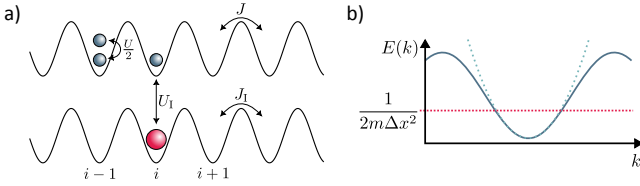


Figure 2. a) Illustration of terms in Hamiltonian eq. (6). The blue circles depict bosons which interact with strength $\frac{U}{2}$ and can hop with amplitude J . The impurity is shown as a red circle. It interacts with the bosons with strength U_I and hops between lattice sites with amplitude J_I . b) Comparison between the sinusoidal dispersion relation of particles in a lattice to that of free particles, with the maximal energy to which both remain comparable.

The discrete Hamiltonian is only a faithful approximation to the continuous model in the low-energy regime. Particles in a lattice possess a sinusoidal dispersion relation while free particles have a parabolic one (see Fig. 2b). The two dispersion relations agree for up to a maximum energy of $\frac{1}{2m\Delta x^2}$ which relates to the hopping amplitude of the bosons J in the discrete system. So the energy per lattice site caused by the interaction between the bosons needs to be lower than the hopping amplitude J . This leads to the condition

$$\tilde{n}_0 U \ll J, \quad (9)$$

where \tilde{n}_0 is the mean particle number per lattice site. In terms of the unitless Tonks parameter γ this can be expressed as

$$\gamma \tilde{n}_0^2 \ll 1. \quad (10)$$

Thus for larger Tonks parameter γ the mean particle number per lattice site \tilde{n}_0 needs to be kept low enough such that the discrete system remains a faithful approximation to the continuous one.

To gauge the effects of the impurity one can look at the polaron energy which gives the energy it takes to immerse an impurity in the Bose gas.

$$E_P = E(g_{IB}) - E(0) \quad (11)$$

where $E(0)$ is the ground-state energy of the system with $g_{IB} = 0$ and $E(g_{IB})$ is the corresponding ground-state energy for a finite boson-impurity interaction. The polaron energy increases with g_{IB} but saturates for large interaction strength once the impurity has displaced all of the condensate at its position.

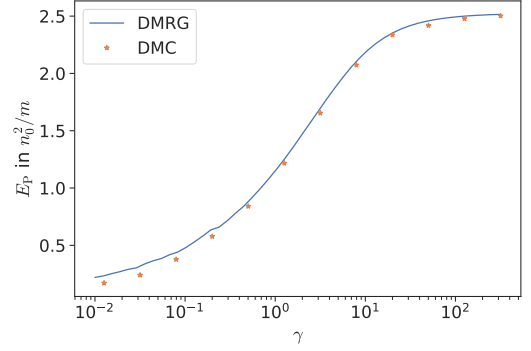


Figure 3. Comparison of the saturated polaron energy ($g_{IB} = \infty$) for an immobile impurity ($M = \infty$) in a Bose gas with $N = 100$ particles from DMRG and diffusion quantum Monte-Carlo results (DMC) from [9].

In order to benchmark our DMRG code we calculated the saturated polaron energy ($g_{IB} = \infty$) of an infinite-mass polaron ($M = \infty$) localized in the center of a 1D quasi condensate with $N = 100$ bosons for varying strength of the boson-boson interaction, quantified by γ , and compared the results with those from diffusion quantum Monte Carlo (DMC) simulations taken from [9], see Fig. 3. The DMC simulations were done for periodic boundary conditions, while the DMRG data are for open boundary conditions, which explains the small difference for small value of γ . Open boundary conditions cause half dark solitons to form on each system edge for $\gamma \ll 1$ and Friedel oscillations for $\gamma \gg 1$ which increase the ground state energy of the system compared to periodic boundary conditions. This was mostly negated here by choosing a system size which is large compared to the characteristic length scale of the system, the healing length $\xi = 1/\sqrt{2g_{n0}m}$ for $\gamma \ll 1$ or the wavelength of Friedel oscillations $2k_F = 2\pi n_0$ for $\gamma \gg 1$. Apart for very small γ values one recognizes excellent agreement.

C. Decoupling mean-field (DMF) ansatz

The Hamiltonian eq. (1) contains both the position and momentum operators, \hat{r} and \hat{p} , of the impurity, which do not commute. This leads to an entanglement between the motional degrees of freedom of the impurity with the boson field. For translationally invariant systems one can solve this problem by a Lee-Low-Pines (LLP) transformation into a co-moving frame [10]. For weak boson-boson interactions and not too small values of the impurity mass the effective Hamiltonian can then be solved rather accurately in a mean-field approximation [12, 13], which due to the LLP transformation takes impurity-boson correlations into account.

Without translational invariance, e.g. if the Bose gas (B) and / or the impurity (I) are subject to some trapping potentials $V_{B,I}(x)$ a LLP transformation does not work. Here often another mean-field ansatz is used, which neglects correlations between impurity and bosons and results in a coupled Gross-Pitaevski and Schrödinger equation for a condensate wavefunction $\phi(x)$ and the impurity wavefunction $\phi_I(x)$, respectively:

$$\begin{aligned} i\partial_t\phi(x,t) = & \left(-\frac{\partial_x^2}{2m} + g_{IB}|\phi_I(x,t)|^2 + \right. \\ & \left. + g|\phi(x,t)|^2 + V_B(x) \right) \phi(x,t), \quad (12) \\ i\partial_t\phi_I(x,t) = & \left(-\frac{\partial_x^2}{2M} + g_{IB}|\phi(x,t)|^2 + V_I(x) \right) \phi_I(x,t). \end{aligned}$$

III. LOCALIZATION-DELOCALIZATION TRANSITION IN A BOX POTENTIAL

We now consider a box potential for bosons and impurity $V_B(x) = V_I(x)$ for which we expect a transition between a delocalized phase, where the impurity is spread out over the whole system, and a localized one, where the impurity is localized at one of the two edges of the system. This is because the energy of an impurity localized at the edge increases as $E_{\text{loc}} \sim \sqrt{g_{IB}}$, while the polaron energy in the bulk scales as $E_p \sim g_{IB}$. Thus for $g_{IB} \rightarrow 0$ no bound state exists which only emerges above a critical value of g_{IB} .

In [30, 31] it has been argued based on a DMF ansatz, eq. (12), that also in a translational invariant, homogeneous system the impurity wavefunction should self-trap in a co-localized distortion of the BEC. The reality of such self-trapped polarons has been subject of discussions [32]. Due to the broken translational invariance in the box potential considered here, the self-trapping would manifest itself in a probability density of the impurity centered in the middle of the trap with a width independent on the trap size L .

In the following we will investigate both localization phenomena for a weakly interacting as well as a strongly interacting Bose gas using DMRG simulations of the full

quantum equations and compare them to numerical solutions and analytical approximations of the DMF equations eq. (12).

A. Localization-delocalization transition in a box potential

We performed DMRG simulations of the ground state of a mobile impurity in a 1D Bose gas in the box potential for different mass ratios M/m and impurity-boson interaction strengths g_{IB} . Results for weak boson-boson interactions, $\gamma = 0.4$, and for the Tonks limit $\gamma = \infty$ are shown in Fig. 4 and Fig. 5, respectively. One recognizes in both cases a sharp transition between a phase where the impurity is delocalized over the trap to a phase where it is localized at one of the two edges. (Note that the true ground state is a superposition of localized states at both edges. Since the energy difference between the symmetric and antisymmetric superpositions vanishes exponentially with increasing system size, the DMRG algorithm converges to a solution on one edge only.) The transition point depends on the boson-boson interaction strength. In the delocalized phase the probability density of the impurity is spread out over the whole system and apart from some corrections at the edges it corresponds to the ground state of the box potential $\sim \cos^2(x\pi/L)$, with L being the length of the box. In the localized phase, on the other hand, the width of the probability distribution becomes independent on system size for large L .

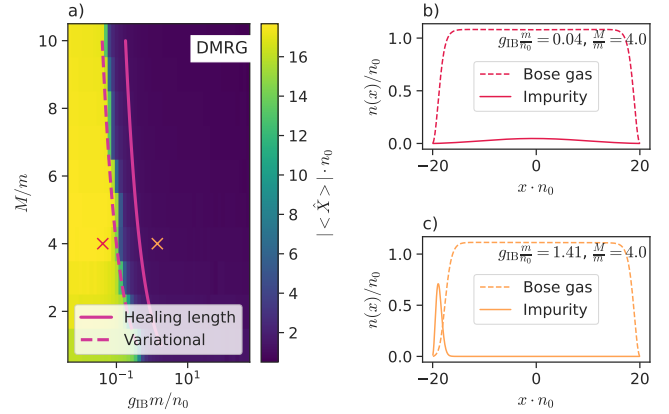


Figure 4. a) Localization-delocalization transition of impurity in a box potential in a weakly interacting Bose gas with Tonks parameter $\gamma = 0.4$ and $N = 40$ particles. Color code describes average position $\langle \hat{X} \rangle$ of impurity. Solid line is the prediction from eq. (15) with $l_0 = \xi$. The dashed line gives the prediction with l_0 from a variational ansatz. b) and c) density distribution corresponding to the two points in Figure a).

A simple estimate for the critical point of the localization-delocalization transition can be obtained as follows: For weak interactions with a Bose gas of density

n_0 the energy of a repulsive polaron is given in lowest-order perturbation by

$$E_p \approx g_{IB} n_0 \quad (13)$$

and thus scales linearly in g_{IB} .

On the other hand the energy of an impurity localized at the edge of the condensate can be estimated from the repulsive potential created by the bosons, whose density increases quadratically close to the potential edge:

For a weakly interacting Bose gas (small γ) the characteristic length scale $l_0 = \eta\xi$ of the harmonic confinement is the healing length ξ of the Bose condensate. The factor $\eta \simeq \mathcal{O}(1)$ accounts for the backaction of the trapped impurity on the density of the condensate near the potential edge, which is relevant in the small- γ regime, due to the large compressibility of the weakly interacting bose gas. The impurity thus experiences an effective potential for small x :

$$V_{\text{eff}}(x) = \begin{cases} \infty & x \leq 0 \\ g_{IB} n_0 \frac{x^2}{2l_0^2} & x > 0. \end{cases}$$

The corresponding oscillator frequency ω follows from $V_{\text{eff}} = \frac{M}{2}\omega^2 x^2$. The ground-state energy of the impurity localized in V_{eff} is thus

$$E_{\text{loc}} \approx \frac{3\omega}{2} = \frac{3}{2} \sqrt{\frac{g_{IB} n_0}{M l_0^2}} \quad (14)$$

which scales only with the square root of g_{IB} . Thus for a small impurity-boson interaction no bound state exists. A localized solution emerges only above a critical value

$$\left. \frac{g_{IB} m}{n_0} \right|_{\text{crit}} = \frac{9}{4\eta^2} \frac{m}{M} \frac{1}{n_0^2 \xi^2} = \frac{9}{2\eta^2} \frac{m}{M} \gamma. \quad (15)$$

In Fig. 4a we have plotted the critical transition line for $\eta = 1$ (solid line). One recognizes that the backaction of the impurity to the condensate needs to be taken into account, which leads to an increased width of the density minimum of the condensate on the left edge, see Fig. 4c.

One can obtain an approximation for the factor η in eq. (15) from a variational coherent-state ansatz considering a half-infinite system with only one edge at $x = 0$. To this end we assume a factorized ground state $|\psi_{\text{gs}}\rangle = |\phi\rangle|\phi_I\rangle$, with

$$\phi(x) = \sqrt{n_0} \tanh(\alpha x). \quad (16)$$

describing the coherent amplitude of the condensate at the edge. $|\phi_I\rangle$ is then the ground state of the impurity in the resulting effective Pöschl-Teller potential, which can be calculated analytically [33]. Minimizing the total energy gives an implicit equation for $\eta = 1/(\sqrt{2}\xi\alpha)$ as function of the mass ratio M/m , the Tonks parameter γ and the normalized Boson-impurity interaction strength $\gamma_{IB} = g_{IB} m/n_0$

$$0 = 1 - \eta^2 - \frac{15}{2} \frac{m}{M} \frac{\gamma^{1/2}}{\eta} + \frac{9}{2} \frac{m}{M} \frac{4\gamma_{IB} \frac{M}{m} \eta^2 + \gamma}{\eta \sqrt{8\gamma_{IB} \frac{M}{m} \eta^2 + \gamma}}. \quad (17)$$

The solution of this equation is shown in Fig. 4 as a dashed line, showing very good agreement.

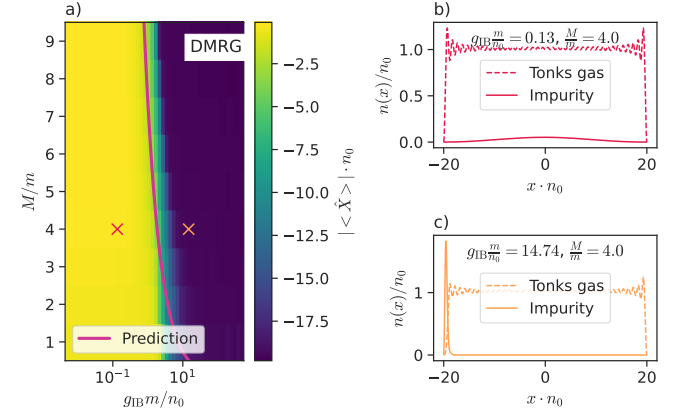


Figure 5. a) Localization-delocalization transition of an impurity in a box potential in a Tonks gas ($\gamma = \infty$, $N = 40$). Solid line is prediction from eq. (19). b) and c) density distribution corresponding to the two points in Figure a).

In the Tonks gas limit ($\gamma \rightarrow \infty$) the hardcore bosons are much less compressible but show Friedel oscillations in the density which also affect the impurity wavefunction in the localized phase. Hardcore bosons can be mapped to free fermions, which due to Pauli exclusion occupy all single-particle states in the trap up to the Fermi energy. Thus the density of the hardcore gas near one of the edges of the box is given by

$$n(x) \approx \frac{2k_F}{\pi} \left(1 - \frac{2 \sin(2k_F x)}{2k_F x} \right), \quad (18)$$

with x being the distance from the edge and $k_F = \pi n_0/2$ is the Fermi momentum. Thus the characteristic length scale l_0 is here $(\sqrt{6}/\pi)n_0^{-1}$ which gives the following estimate for the critical value of the localization-delocalization transition:

$$\left. \frac{g_{IB} m}{n_0} \right|_{\text{crit}} = \frac{9}{2} \frac{m}{M} \frac{\pi^2}{6}. \quad (19)$$

In Fig. 5a.) we have also plotted this value for comparison and one recognizes reasonable good agreement. Due to the smaller compressibility of the Tonks gas, the localization transition is shifted to higher values of g_{IB} .

B. Absence of self-localization in a weakly interacting Bose gas

We now compare the results from DMRG simulations with solutions of the DMF equations eq. (12). In Fig. 6 we show the average position of the impurity as function of the mass ratio M/m and the impurity-boson interaction g_{IB} from DMRG (a) and DMF (b) simulations for

$\gamma = 0.4$, i.e. for weak boson-boson interactions. Figure (c) shows a cut for two mass ratios. Since the Tonks parameter is still small, we expect the mean-field simulations to provide good results. And indeed one recognizes that the localization-delocalization transition to the edge of the trap is reasonably well captured by the DMF approach. However, for small mass ratios $\frac{M}{m} < 1.3$ there is an area of coupling strengths around $g_{\text{IB}} m/n_0 \approx 0.5$ where there is a self-localisation of the impurity in the middle of the box. Importantly the width of the impurity distribution in this region is much smaller than the box size, as can be seen in Fig. 7, where we compared the width of the impurity distribution from DMRG and DMF simulations.

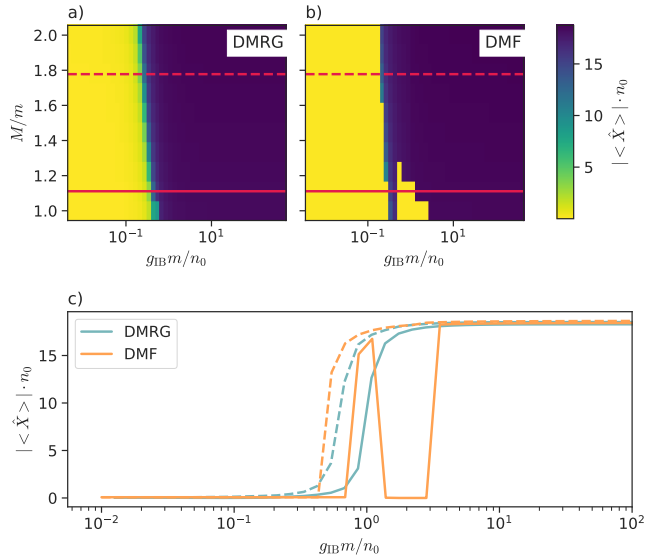


Figure 6. Comparison between average impurity position $\langle \hat{X} \rangle$ calculated from DMRG and decoupling mean field (DMF) calculations for a Bose gas with $\gamma = 0.4$ and $N = 40$. a) Colorplot of $\langle \hat{X} \rangle$ as function of mass ratios M/m and boson-impurity interaction g_{IB} obtained by DMRG. Red lines show cuts which are plotted in c). b) The same obtained from decoupling mean field simulations (DMF). c) Cuts in a) for two mass ratios, solid and dashed line correspond to each other.

In Fig. 8 we have plotted the density distributions of bosons and impurity in the box potential for a mass ratio $M/m = 1$ for different values of g_{IB} inside the region of self trapping predicted by DMF. Also shown is the analytic prediction from [31] for the impurity probability density in the self-trapping regime

$$|\phi_{\text{I}}(x)|_{\text{TF}}^2 = \frac{1}{2\lambda} \text{sech}^2\left(\frac{x}{\lambda}\right) \quad (20)$$

with $\lambda = \sqrt{2/\gamma^3} (g/g_{\text{IB}})^2 (m/M) n_0^{-1}$ being the localization length, which holds in the Thomas Fermi limit, i.e. for $\lambda \gg n_0^{-1}$.

The self-localisation is an artifact of the decoupling approximation and is not present in the full quan-

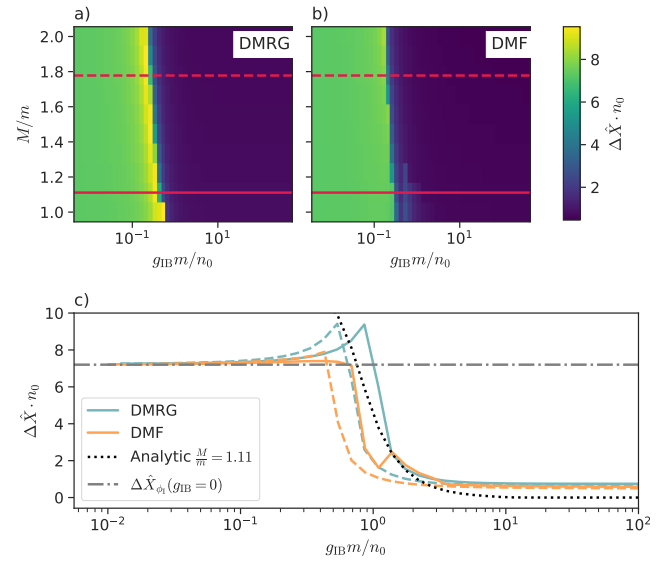


Figure 7. Comparison between the variance of the impurity $\langle \hat{X} \rangle$ calculated from DMRG and decoupling mean field calculations for a Bose gas with $\gamma = 0.4$ and $N = 40$. a) Colorplot of variance from DMRG simulations as function of mass ratios M/m and boson-impurity interaction g_{IB} . Red lines show cuts which are plotted in c). b) The same obtained from decoupling mean field simulations (DMF). c) Cuts in a) for two mass ratios, solid and dashed line correspond to each other. The grey dashed-dotted line shows the spatial width of the impurity expected for $g_{\text{IB}} = 0$, which is given by the ground-state density distribution of a particle in a box $\cos^2(x\pi/L)$. The black dotted line shows the self-localization length λ predicted in DMF for $\frac{M}{m} = 1.11$.

tum approach. This is because boson-impurity correlations, which are neglected in DMF, suppress the self-localization [32].

IV. HEAVY POLARON IN STRONGLY INTERACTING BOSE GAS

A characteristic quantity of the polaron is the energy E_{P} needed to immerse an impurity into the Bose gas $E_{\text{P}} = E(g_{\text{IB}} \neq 0) - E(g_{\text{IB}} = 0)$. Here $E(g_{\text{IB}} = 0)$ is the ground state energy of the system without Bose-impurity-interaction and $E(g_{\text{IB}} \neq 0)$ with Bose-impurity-interaction.

For a heavy impurity and a weakly interacting Bose gas, $\gamma \ll 1$, with periodic boundary conditions, a mean-field approximation to the polaron Hamiltonian after a Lee-Low-Pines transformation gives a rather accurate prediction of the polaron energy [11, 12, 15]:

$$E_{\text{P}} = \frac{4}{3} n \bar{c} \left[1 + \frac{3}{2} \chi + \chi^3 - (1 + \chi^2)^{3/2} \right], \quad (21)$$

where the dimensionless parameter $\chi = g_{\text{IB}}/(2\sqrt{2}gn\bar{\xi})$ characterizes the impurity-boson interaction strength. If

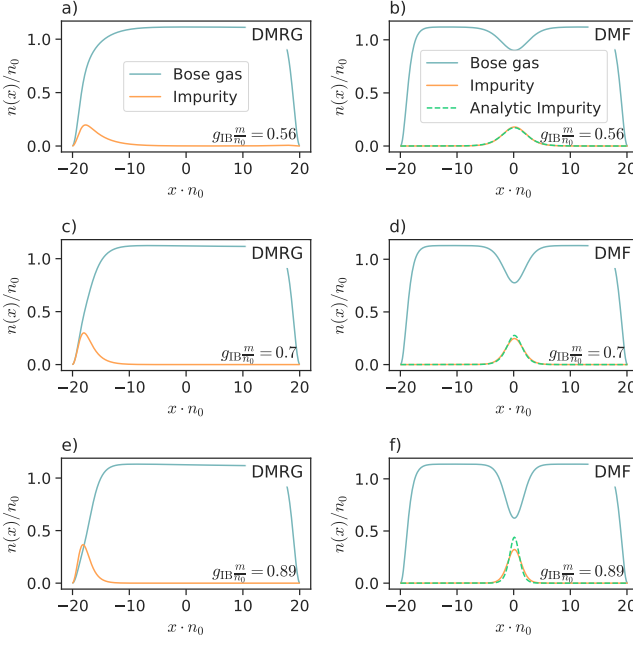


Figure 8. *Left:* Density distribution of Bose gas and impurity for different g_{IB} (written in the lower right) from DMRG simulations. *Right:* The same from mean-field calculations compared to the analytic prediction for a self-trapped polaron, eq. (20). Parameters of the bose gas are $\gamma = 0.4$, $M/m = 1$ and $N = 40$.

$|\chi| \gtrsim 1$ the condensate undergoes substantial deformation. $\bar{\xi} = \xi \sqrt{m/m_r}$ and $\bar{c} = \sqrt{m/m_r}c$ are the rescaled healing length and speed of sound respectively. n is the boson density without impurity and $m_r = (Mm)/(M + m)$ is the reduced mass.

In the following we will employ DMRG simulations to calculate the polaron energy in a strongly interacting Bose gas.

A. Polaron energy and density profile

For an impurity whose mass is much larger then that of the bosons ($\frac{M}{m} \gg 1$) the kinetic energy of the impurity can be neglected. The resulting effective Hamiltonian then reduces to a interacting boson problem in an external δ potential

$$\hat{H} = \int dx \hat{\phi}^\dagger(x) \left(-\frac{\partial_x^2}{2m} + \frac{g}{2} \hat{\phi}^\dagger(x) \hat{\phi}(x) + g_{IB} \delta(x) \right) \hat{\phi}(x). \quad (22)$$

Figures 9 and 10 show the polaron energy in a weakly ($\gamma = 0.4$) and a strongly ($\gamma = 20$) interacting, trapped 1D Bose gas, calculated by DMRG simulations. For $\gamma = 0.4$ the analytic prediction from eq. (21) is plotted for comparison, showing very good agreement. Also shown are plots for the boson density for two different values of g_{IB}

g_{IB} . In the first case the characteristic size of the condensate depletion around the fixed position of the impurity is given by the healing length, in the second case by the wavelength of the Friedel oscillations of the (almost) Tonks gas. One recognizes that in both cases the polaron energy saturates for increasing g_{IB} , which happens when the density of the Bose gas at the position of the impurity approaches zero.

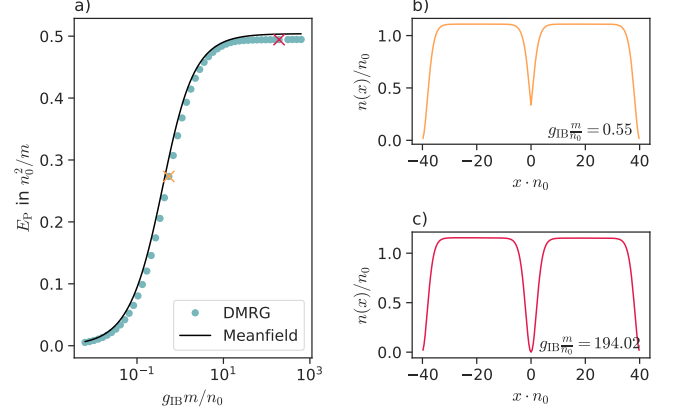


Figure 9. Polaron in weakly interacting 1D Bose gas with $\gamma = 0.1$, $M = \infty$ and $N = 80$: a) polaron energy as function of impurity-boson interaction calculated from DMRG simulations and Meanfield approximations in the LLP frame [11, 12], b), c) wavefunction for two different values of g_{IB} (written in the lower right) in a box and impurity fixed at $x = 0$.

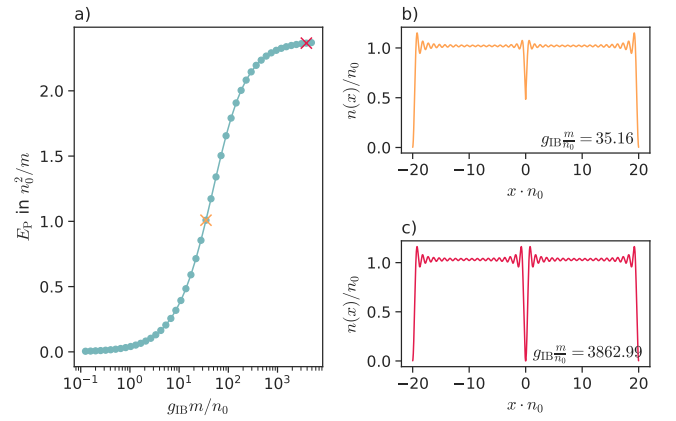


Figure 10. Polaron in strongly interacting 1D Bose gas with $\gamma = 20$ and $N = 80$ particles in a finite box and $M = \infty$: a) polaron energy as function of impurity-boson interaction, b), c) wavefunction for two different values of g_{IB} (written in the lower right) in a box potential and impurity fixed at $x = 0$.

B. Analytic approximation of the polaron energy for $\gamma \gg 1$

For large but finite values of γ one can derive semi-analytic expressions for the polaron energy. As shown by Girardeau [29], bosons with s -wave contact interactions are dual to spin-polarized fermions with p -wave interactions and both can be mapped onto each other by the well-known boson-fermion mapping [29, 34]: The bosonic Hamiltonian eq. (22) can be written as a fermionic Hamiltonian

$$\hat{H}_F = \int dx \hat{\psi}^\dagger(x) \left(-\frac{\partial_x^2}{2m} + g_{IB} \delta(x) \right) \hat{\psi}(x) + \frac{g_F}{2} \iint dx dy \hat{\psi}^\dagger(x) \hat{\psi}^\dagger(y) \overleftarrow{\frac{\partial}{\partial z}} \delta(z) \overrightarrow{\frac{\partial}{\partial z}} \hat{\psi}(y) \hat{\psi}(x), \quad (23)$$

where $z = x - y$ and $\hat{\psi}$ are fermionic field operators. The arrows above the derivatives mean that in the case of the arrow to the left, the derivative has to be applied to the function on the left of it and for the arrow to the right on the function to the right. The p -wave interaction strength g_F is then related to the bosonic interaction strength g via

$$g_F = -\frac{4}{g}. \quad (24)$$

This means a strongly s -wave interacting Bose gas maps to a weakly p -wave interacting Fermi gas and vice versa.

The boson-fermion mapping provides an elegant way to find approximate analytic expressions for the polaron energy in a strongly interacting Bose gas with $\gamma \gg 1$ perturbatively in $|g_F| \sim 1/\gamma$. To this end we first have to calculate the single particle solutions of free fermions with a infinitely heavy impurity at $x = 0$ for open boundary conditions (OBCs). This system is described by the Hamiltonian

$$\hat{H}_F^0 = \int_{-L/2}^{L/2} dx \hat{\psi}^\dagger(x) \left(-\frac{\partial_x^2}{2m} + g_{IB} \delta(x) \right) \hat{\psi}(x). \quad (25)$$

This means we need to solve the problem of non-interacting fermions trapped in a infinitely deep box potential (OBC's) with a delta potential in the middle.

The single particle solutions are given by

$$\varphi_l(x) = a_l \text{sgn}(x)^l \sin \left(k_l \left(|x| - \frac{L}{2} \right) \right) \quad (26)$$

where l is an integer and the wave numbers k_l have to be numerically calculated from the boundary condition at the delta potential

$$0 = \frac{k_l}{2m} (1 + (-1)^l) + g_{IB} \tan \left(k_l \frac{L}{2} \right). \quad (27)$$

The ground state $|\psi\rangle$ and the ground state energy E

can be written as

$$|\psi\rangle = \int dx_1 \dots \int dx_N \varphi_1(x_1) \dots \varphi_N(x_N) \times \hat{\psi}^\dagger(x_1) \dots \hat{\psi}^\dagger(x_N) |0\rangle, \quad (28)$$

$$E = \sum_{l=1}^N \frac{k_l^2}{2m}. \quad (29)$$

The second line in eq. (23) can now be treated as perturbation, i.e. $\hat{H}_F = \hat{H}_F^0 + \hat{H}_1$ and the first-order energy correction ΔE_1 reads

$$\Delta E_1 = \langle \psi | \hat{H}_1 | \psi \rangle \quad (30)$$

$$= \frac{g_F}{2} \sum_{l,n \neq l}^N \frac{a_l^2 a_n^2 k_l}{4k_n} \left[(k_n - k_n \cos(k_n L)) \sin(k_l L) + k_l (k_n L - \sin(k_n L)) \right]. \quad (31)$$

Fig. 11 shows a comparison of the polaron energies as function of g_{IB} from first order perturbation in $1/\gamma$ with numerical DMRG results. One recognizes rather good agreement even down to $\gamma = 20$.

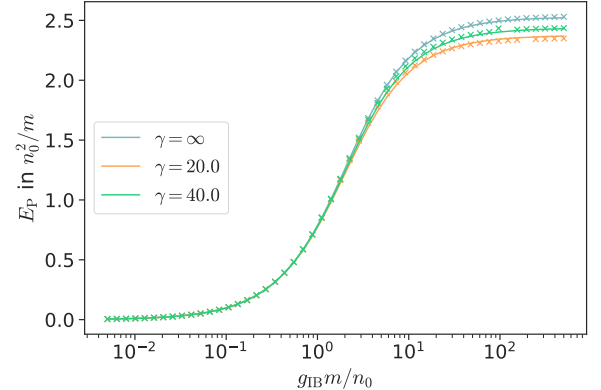


Figure 11. Comparison of perturbative analytic approximation to polaron energy (solid lines) with DMRG results (crosses) for a strongly interacting 1D Bose gas with $\gamma = 20, 40, \infty$ and $N = 80$ particles respectively.

V. POLARON INTERACTION IN A STRONGLY INTERACTING BOSE GAS IN THE BORN-OPPENHEIMER LIMIT

Interactions between particles mediated by a many-body environment play an important role in condensed-matter systems. Examples include the Ruderman-Kittel-Kasuya-Yosida (RKKY) interaction of spins in a Fermi liquid [2-4] and Cooper pairing of electrons [5]. The mechanism responsible for these interactions is the same as what causes the formation of quasi-particles such as the polaron. Even if the impurities don't interact directly

with each other, as we will assume here, they do so by their coupling to the condensate. If the impurities get close to each other they expel the Bose gas between them and the surrounding gas pushes the impurities together. This causes an effective attractive interaction which in itself can lead to the formation of bound states called bi-polaron states. The understanding of bi-polarons is one of the key questions of many-body physics. They are suspected to be key for high-temperature superconductivity [35–37] and phenomena such as the electric conductivity of polymers [38–42] or organic magneto-resistance [43].

For a weakly interacting Bose gas ($\gamma \ll 1$) a mean-field ansatz in the LLP frame can be used to obtain semi-analytic expressions of the interaction potential at short distances, which agree very well with quantum Monte-Carlo simulations [13]. The mean field approach does not describe the Casimir-like contributions arising from the exchange of virtual phonons [44–46], which give however only important corrections in the already small tails of the interaction potential.

In this section we investigate the interaction between Bose polarons in a strongly-interacting 1D quasi condensate numerically by DMRG simulations. Since DMRG is not well suited for periodic boundary conditions, we again assume a confinement of the Bose gas to a box potential. As long as the distance of the impurities from the edges of the box is much larger than the healing length or the Fermi wavelength, boundary effects can be neglected. For the same reason our simulations, although in principle suitable, do not allow to accurately extract the far tails of the interaction potential, dominated by virtual phonon exchange. As discussed in the Appendix, the DMRG simulations reproduce the semi-analytical results from Ref.[13] obtained in mean-field theory for small values of γ .

In the following we calculate the polaron interaction potential in Born-Oppenheimer approximation where $\frac{M}{m} \gg 1$. Here the impurities do not possess kinetic energy and are localized in space. By varying their distance r one can determine the polaron interaction potential $V(r)$ from

$$V(r) = E_{lr}(r) - E_l(r) - E_r(r) + E_0. \quad (32)$$

Here $E_{lr}(r)$ is the ground state energy with both impurities present, E_l (E_r) the ground state energy with only the left (right) impurity, and E_0 is the ground state energy of the Bose gas without any impurities. In the case of two impurities and for $\frac{M}{m} \gg 1$ the Hamiltonian becomes

$$\hat{H}_B = \int dx \hat{\phi}^\dagger(x) \left(-\frac{\partial_x^2}{2m} + \frac{g}{2} \hat{\phi}^\dagger(x) \hat{\phi}(x) \right) \hat{\phi}(x) + \hat{\phi}^\dagger(x) \left\{ g_{IB} \left[\delta \left(x + \frac{r}{2} \right) + \delta \left(x - \frac{r}{2} \right) \right] \right\} \hat{\phi}(x), \quad (33)$$

where the two impurities are described by the delta potentials at $\frac{r}{2}$ and $-\frac{r}{2}$.

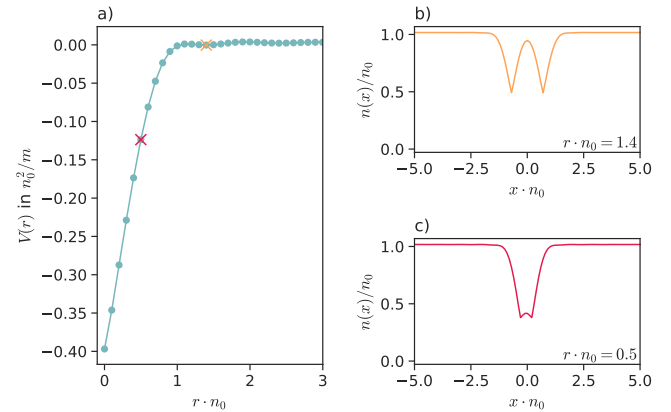


Figure 12. *Left:* Interaction potential of heavy impurities in a bose gas with $\gamma = 4$ and $N = 100$ particles and bose-impurity interaction strength $g_{IBM}/n_0 = 1.08$. *Right:* Density of Bose gas at the two separations indicated in left picture as crosses in the corresponding color.

Fig. 12 shows the short-distance behaviour of $V(r)$ for a medium-sized Tonks parameter $\gamma = 4$ as well as density distributions of the bosons for two different separations r between the impurities. One recognizes a linear potential for small distances similar to the results of [13] for a weakly interacting Bose gas. The effective potential becomes attractive as soon as the Bose gas between the polarons is substantially diminished. The pressure from the atoms to the left and to the right of the polaron pair then causes a constant force and thus a linear interaction potential.

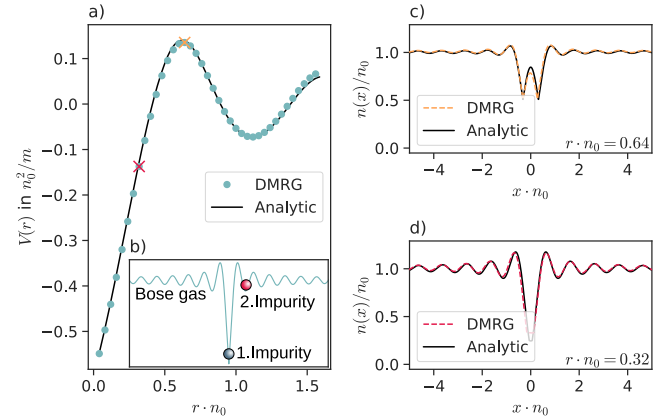


Figure 13. *Left:* Interaction potential of heavy impurities in the Tonks-gas limit $\gamma = \infty$, $N = 80$ and $g_{IBM}/n_0 = 1.58$. Insert illustrates origin of oscillatory potential. Also shown is the analytic prediction (black line) of the interaction potential obtained from mapping to free fermions in PBC. *Right:* Density of Bose gas at the two separations indicated in left picture as crosses in the corresponding color.

For large values of γ on the other hand oscillations appear in the polaron potential, as can be seen in Fig. 13.

The frequency of these oscillations is that of the Friedel oscillations caused by the polarons themselves. As shown in Fig. 13b.), once a single impurity is introduced into the system it causes density oscillation and the second impurity has to displace a smaller or a larger amount of bosons and therefore needs less or more energy to form a polaron. The resulting energy modulations reflect themselves in the polaron potential.

It can also be seen, that the gradient of the potential increases with the Tonks parameter. This is the case since the force results from the surrounding Bose gas pushing against the polarons. For a stronger interacting Bose gas the resulting larger quantum pressure in the gas exerts a bigger force on the polarons.

The interaction potential in the Tonks gas limit can also be obtained directly. To this end we have to calculate the energy of a free Fermi gas (Tonks gas) in a box with periodic boundary conditions in the presence of one or two δ -potentials with strength g_{1B} at positions $x = \pm r/2$, which is an elementary quantum mechanics problem. The interaction potential can then be obtained from the total energy E_{1r} of the Tonks gas in the presence of two δ -potentials, the energy E_1 of a single δ -potential, and the energy without impurities E_0 :

$$V(r) = E_{1r} - 2E_1 + E_0. \quad (34)$$

As can be seen in Fig. 13 the bipolaron potential as well as the density distribution of the Tonks gas obtained in this way compare quite well with the DMRG simulations.

VI. SUMMARY

In the present paper we studied the ground state of a mobile impurity in a one-dimensional Bose gas in a box potential for arbitrary impurity-boson and boson-boson interactions. To fully account for quantum effects, which are particularly important in the limit of large Tonks parameters γ , we performed numerical simulations of a discretized effective lattice model using the density-matrix renormalization group.

Mean-field approaches to the Bose polaron have been shown to provide accurate descriptions for heavy impurities ($M/m \geq 3$) and weak boson-boson interactions ($\gamma \leq 1$), if the back-action of the impurity to the condensate is properly taken into account. We here showed that it is important to also keep impurity-boson correlations in the mean-field description, in agreement with recent findings in [32]. In translationally invariant systems or for harmonic trapping of both impurity and bosons this can be achieved by a Lee-Low-Pines transformation of the original Hamiltonian, reducing the interaction problem to one of interacting bosons in a delta-Potential, before applying a mean-field approximation. On the other hand, a commonly used mean-field approach, where condensate and impurity are described by a factorized impurity-boson c-number wavefunction, leading to a coupled Gross-Pitaevski – Schrödinger equation, disregards

such correlations. As a consequence such an approach predicts the existence of a self-trapped polaron for arbitrarily small impurity-boson couplings in a homogeneous 1D gas, where the impurity is localized in a distortion of the condensate created by the impurity. A comparison of the predictions of such a decoupling mean-field (DMF) theory with exact DMRG results shows that the self-trapped solution is an artifact of the DMF approach.

As DMRG simulations allow us to consider Bose polarons in a strongly-interacting Bose gas, we furthermore calculated the polaron energy in this regime and derived analytical approximations for large but finite Tonks parameters $\gamma \gg 1$ by using the mapping to weakly interacting fermions. Finally we numerically calculated the short-distance interaction potential between two impurities in Born-Oppenheimer approximation for arbitrarily strong boson-boson interactions. For small Tonks parameter $\gamma \leq 1$ we verified the results of [13] were a linear short-distance behaviour was predicted. In the strong interaction limit $\gamma \gg 1$ we found oscillatory modulations in the potential, which can be interpreted as the effect of Friedel-type oscillations in the condensate density caused by one impurity affecting the polaron formation of the second impurity.

Acknowledgement

The authors gratefully acknowledge financial support by the DFG through SFB/TR 185, Project No.277625399.

APPENDIX

A. Discretization of continuous gas: Higher order representation of the second order derivatives

Let us comment on some techniques to improve the numerical simulations. It turns out to be beneficial for the convergence of the DMRG algorithm to use a higher order representation of the second order derivatives. So

$$\partial_x^2 \hat{\phi}(x) \approx \frac{-\frac{1}{12} \hat{a}_{i-2} + \frac{4}{3} \hat{a}_{i-1} - \frac{5}{2} \hat{a}_i + \frac{4}{3} \hat{a}_{i+1} - \frac{1}{12} \hat{a}_{i+2}}{\Delta x}. \quad (35)$$

By inserting these transformations in continuous Hamiltonian one arrives at

$$\begin{aligned} \hat{H} = & \sum_i \frac{1}{12} J \left(\hat{a}_i^\dagger \hat{a}_{i+2} + \text{h.c.} \right) - \frac{4}{3} J \left(\hat{a}_i^\dagger \hat{a}_{i+1} + \text{h.c.} \right) \\ & + \frac{5}{2} J \left(\hat{a}_i^\dagger \hat{a}_i + \text{h.c.} \right) + U \hat{a}_i^\dagger \hat{a}_i^\dagger \hat{a}_i \hat{a}_i \\ & \frac{1}{12} J_I \left(\hat{b}_i^\dagger \hat{b}_{i+2} + \text{h.c.} \right) - \frac{4}{3} J_I \left(\hat{b}_i^\dagger \hat{b}_{i+1} + \text{h.c.} \right) \\ & + \frac{5}{2} J_I \left(\hat{b}_i^\dagger \hat{b}_i + \text{h.c.} \right) + U_I \hat{b}_i^\dagger \hat{a}_i^\dagger \hat{a}_i \hat{b}_i. \end{aligned} \quad (36)$$

As compared to a lattice Hamiltonian derived from eq. (5), the above expression eq. (36) contains longer-range hopping terms. These help the DMRG algorithm to establish correlations and therefore the algorithm is able to reach the ground state faster.

B. Comparison of polaron-polaron interaction potential to mean-field result

In the case of a weakly interacting Bose gas with $\gamma \ll 1$ the interaction potential between two Bose polarons in Born-Oppenheimer approximation can be determined semi-analytical [13]. One finds for repulsive interactions

$$V(r) = gn_0^2 r \left(\frac{1}{2} - \frac{4+2\nu}{3(\nu+1)^2} \right) + \frac{4}{3} \frac{gn_0^2 \bar{\xi}}{\sqrt{1+\nu}} \left\{ \sqrt{2\nu+2} + 2E(am(u, \nu), \nu) - \frac{\sqrt{\nu}^3}{1+v} cd(u, \nu)^3 [1 + \sqrt{\nu} sn(u, \nu)] - \sqrt{\nu} cd(u, \nu) \left[\frac{3}{2} + \frac{1+2\nu}{1+\nu} \sqrt{\nu} sn(u, \nu) \right] \right\}, \quad (37)$$

where $u = r/(2\bar{\xi}\sqrt{1+\nu})$ is a normalized distance, $E(x, \nu)$ is the incomplete elliptic integral of the second kind, $cd(x, \nu)$ and $sn(x, \nu)$ are Jacobi elliptic functions and $am(x, \nu)$ is the amplitude of these functions [47]. The dimensionless parameter $\nu = \nu(r, \eta)$ with $|\nu| < 1$ is given implicitly by

$$2 \frac{|\eta|}{n_0 \bar{\xi}} \frac{\sqrt{\nu(\nu+1)}}{(1-\nu)} cn(u, \nu) dn(u, \nu) = [1 + \sqrt{\nu} sn(u, \nu)]^2,$$

involving the Jacobi elliptic sn , cn , and dn functions and $\eta = g_{IB}/g > 0$. In general, this equation has several solutions, however the physically relevant one is that with the largest ν .

In Fig. 14 we have shown a comparison of the DMRG results (full line) with the above prediction (dashed line).

- [1] A. S. Alexandrov and J. T. Devreese, *Advances in Polaron Physics*, Vol. 159 (Springer-Verlag, Berlin, 2010).
- [2] M. A. Ruderman and C. Kittel, Indirect exchange coupling of nuclear magnetic moments by conduction electrons, *Phys. Rev.* **96**, 99 (1954).
- [3] T. Kasuya, A Theory of Metallic Ferro- and Antiferromagnetism on Zener's Model, *Progress of Theoretical Physics* **16**, 45 (1956).
- [4] K. Yosida, Magnetic properties of cu-mn alloys, *Phys. Rev.* **106**, 893 (1957).
- [5] L. N. Cooper, Bound electron pairs in a degenerate fermi gas, *Phys. Rev.* **104**, 1189 (1956).
- [6] L. Landau, Über die Bewegung der Elektronen in Kristallgitter, *Phys. Z. Sowjetunion* **3**, 644 (1933).
- [7] S. I. Pekar, Effective mass of a polaron, *Zh. Eksp. Teor. Fiz.* **16**, 335 (1946).
- [8] H. Fröhlich, Electrons in lattice fields, *Adv. Phys.* **3**, 325 (1954).
- [9] F. Grusdt, G. E. Astrakharchik, and E. Demler, Bose polarons in ultracold atoms in one dimension: beyond the fröhlich paradigm, *New Journal of Physics* **19**, 103035 (2017).
- [10] T. D. Lee, F. E. Low, and D. Pines, The motion of slow electrons in a polar crystal, *Phys. Rev.* **90**, 297 (1953).
- [11] A. G. Volosniev and H.-W. Hammer, Analytical approach to the bose-polaron problem in one dimension, *Phys. Rev. A* **96**, 031601 (2017).
- [12] J. Jager, R. Barnett, M. Will, and M. Fleischhauer, Strong-coupling bose polarons in one dimension: Condensate deformation and modified bogoliubov phonons, *Phys. Rev. Res.* **2**, 033142 (2020).
- [13] M. Will, G. E. Astrakharchik, and M. Fleischhauer, Polaron interactions and bipolarons in one-dimensional bose gases in the strong coupling regime, *Phys. Rev. Lett.* **127**, 103401 (2021).

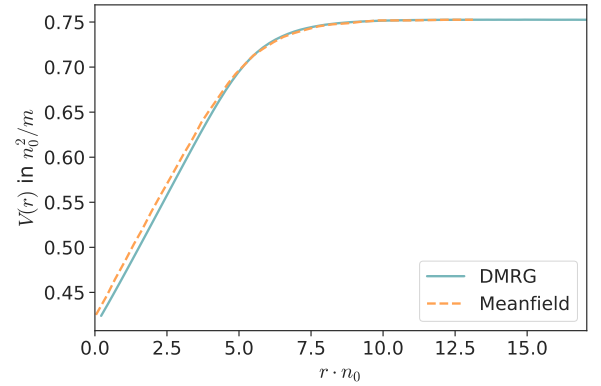


Figure 14. Comparison of polaron-polaron interaction potential from Meanfield calculations [13] (dashed lines) and from DMRG simulations (solid lines) for a boson-impurity interaction strength $g_{IB} \frac{m}{n_0} = 1.25$ and a weakly interacting Bose gas with $\gamma = 1/8$ and $N = 80$ particles.

- [14] M. Will and M. Fleischhauer, Dynamics of polaron formation in 1d bose gases in the strong-coupling regime, *New Journal of Physics* **25**, 083043 (2023).
- [15] G. Panochko and V. Pastukhov, Mean-field construction for spectrum of one-dimensional bose polaron, *Annals of Physics* **409**, 167933 (2019).
- [16] E. Timmermans, Phase separation of bose-einstein condensates, *Physical review letters* **81**, 5718 (1998).
- [17] D. Lee and J. Gunn, Polarons and bose decondensation: A self-trapping approach, *Physical Review B* **46**, 301 (1992).

[18] F. Cucchietti and E. Timmermans, Strong-coupling polarons in dilute gas bose-einstein condensates, *Physical review letters* **96**, 210401 (2006).

[19] K. Sacha and E. Timmermans, Self-localized impurities embedded in a one-dimensional bose-einstein condensate and their quantum fluctuations, *Physical Review A—Atomic, Molecular, and Optical Physics* **73**, 063604 (2006).

[20] R. M. Kalas and D. Blume, Interaction-induced localization of an impurity in a trapped bose-einstein condensate, *Physical Review A—Atomic, Molecular, and Optical Physics* **73**, 043608 (2006).

[21] M. Bruderer, W. Bao, and D. Jaksch, Self-trapping of impurities in bose-einstein condensates: Strong attractive and repulsive coupling, *Europhysics Letters* **82**, 30004 (2008).

[22] A. Blinova, M. Boshier, and E. Timmermans, Two polaron flavors of the bose-einstein condensate impurity, *Physical Review A—Atomic, Molecular, and Optical Physics* **88**, 053610 (2013).

[23] D. Brewer, U. of Sussex, I. U. of Pure, and A. Physics, *Quantum Fluids: Proceedings* (North-Holland Publishing Company, 1966).

[24] J. P. Hernandez, Electron self-trapping in liquids and dense gases, *Reviews of modern physics* **63**, 675 (1991).

[25] U. Schollwöck, The density-matrix renormalization group in the age of matrix product states, *Annals of Physics* **326**, 96 (2011), january 2011 Special Issue.

[26] M. Fishman, S. R. White, and E. M. Stoudenmire, The ITensor Software Library for Tensor Network Calculations, *SciPost Phys. Codebases* , 4 (2022).

[27] N. D. Mermin and H. Wagner, Absence of ferromagnetism or antiferromagnetism in one- or two-dimensional isotropic heisenberg models, *Phys. Rev. Lett.* **17**, 1133 (1966).

[28] P. C. Hohenberg, Existence of long-range order in one and two dimensions, *Phys. Rev.* **158**, 383 (1967).

[29] M. Girardeau, Relationship between Systems of Impenetrable Bosons and Fermions in One Dimension, *Journal of Mathematical Physics* **1**, 516 (1960), https://pubs.aip.org/aip/jmp/article-pdf/1/6/516/19055341/516_1_online.pdf.

[30] F. M. Cucchietti and E. Timmermans, Strong-coupling polarons in dilute gas Bose-Einstein condensates, *Phys. Rev. Lett.* **96**, 10.1103/PhysRevLett.96.210401 (2006).

[31] M. Bruderer, W. Bao, and D. Jaksch, Self-trapping of impurities in bose-einstein condensates: Strong attractive and repulsive coupling, *Europhysics Letters* **82**, 30004 (2008).

[32] L. Zschetsche and R. E. Zillich, Suppression of polaron self-localization by correlations, *Physical Review Research* **6**, 023137 (2024).

[33] M. M. Nieto, Exact wave-function normalization constants for the $b_0 \tanh z - u_0 \cosh^{-2} z$ and pöschl-teller potentials, *Physical Review A* **17**, 1273 (1978).

[34] T. Cheon and T. Shigehara, Fermion-boson duality of one-dimensional quantum particles with generalized contact interactions, *Physical review letters* **82**, 2536 (1999).

[35] A. S. Alexandrov and A. B. Krebs, Polarons in high-temperature superconductors, *Phys. Usp.* **35**, 345 (1992).

[36] N. Mott, Polaron models of high-temperature superconductivity, *Phys. C Supercond.* **205**, 191 (1993).

[37] A. S. Alexandrov and N. F. Mott, Bipolarons, *Reports on Progress in Physics* **57**, 1197 (1994).

[38] J. L. Bredas and G. B. Street, Polarons, bipolarons, and solitons in conducting polymers, *Accounts of Chemical Research* **18**, 309 (1985).

[39] S. Glenis, M. Benz, E. LeGoff, J. L. Schindler, C. R. Kannevurf, and M. G. Kanatzidis, Polyfuran: a new synthetic approach and electronic properties, *Journal of the American Chemical Society* **115**, 12519 (1993).

[40] M. N. Bussac and L. Zuppiroli, Bipolaron singlet and triplet states in disordered conducting polymers, *Phys. Rev. B* **47**, 5493 (1993).

[41] M. Fernandes, J. Garcia, M. Schultz, and F. Nart, Polaron and bipolaron transitions in doped poly(p-phenylene vinylene) films, *Thin Solid Films* **474**, 279 (2005).

[42] I. Zozoulenko, A. Singh, S. K. Singh, V. Gueskine, X. Crispin, and M. Berggren, Polarons, bipolarons, and absorption spectroscopy of pedot, *ACS Applied Polymer Materials* **1**, 83 (2019).

[43] P. A. Bobbert, T. D. Nguyen, F. W. A. van Oost, B. Koopmans, and M. Wohlgemant, Bipolaron mechanism for organic magnetoresistance, *Phys. Rev. Lett.* **99**, 216801 (2007).

[44] M. Schecter, D. M. Gangardt, and A. Kamenev, Quantum impurities: from mobile Josephson junctions to depletons, *New J. Phys.* **18**, 065002 (2016).

[45] B. Reichert, A. Petković, and Z. Ristivojevic, Field-theoretical approach to the Casimir-like interaction in a one-dimensional Bose gas, *Phys. Rev. B* **99**, 205414 (2019).

[46] A. Petković and Z. Ristivojevic, Mediated interaction between polarons in a one-dimensional bose gas, *Physical Review A* **105**, L021303 (2022).

[47] D. F. Lawden, *Elliptic Functions and Applications* (Applied Mathematical Sciences, 1989).